Celal Bayar University Journal of Science

Voltammetric Determination of Hydroxychloroquine Used in the Treatment of COVID-19 at MWCNT Modified Pencil Graphite Electrode

Sultan Hasankahyaoğlu[1], Şevval Sazlık[1], İrem Demir[1], Selen Ayaz[1], Didem Giray Dilgin[2]*

[1]Çanakkale Onsekiz Mart University, Faculty of Science, Department of Chemistry, 17020, Çanakkale, Türkiye
[2]Çanakkale Onsekiz Mart University, Faculty of Education, Department of Secondary Science and Mathematics Education, TR-17010 Çanakkale, Türkiye
* didemgiray@comu.edu.tr
* Orcid No: 0000-0002-3487-3470

Received: May 26, 2025
Accepted: July 19, 2025
DOI: 10.18466/cbayarfbe.1705373

Abstract

COVID-19, the most significant pandemic of the 21st century, has prompted the use of various drugs to slow down the viral process in patients infected with it. One of these drugs is hydroxychloroquine, and due to its importance and frequent use in the treatment of COVID-19, its rapid, accurate and inexpensive determination in biological or pharmaceutical samples is very important. In this study, the electrochemical behavior of hydroxychloroquine was investigated, and voltammetric determination of hydroxychloroquine was performed with a pencil graphite electrode modified with multi-walled carbon nanotubes. Scanning electron microscopy images were used to examine the surfaces of both the regular pencil graphite electrode and the modified one with multi-walled carbon nanotube. Cyclic voltammetric measurements showed that hydroxychloroquine was irreversibly oxidized at approximately +700 and +900 mV in Britton Robinson buffer solution at pH 10.0. Considering these oxidation peaks, differential pulse voltammetric determination of hydroxychloroquine was carried out under optimized conditions. A linear response was obtained from the multi-walled carbon nanotube-modified pencil graphite electrode in the range of 0.1 to 200 $\mu molL^{-1}$ for peaks at both +700 mV and +900 mV with detection limits of 0.04 and 0.05 $\mu molL^{-1}$, respectively. The method was tested on the real tablet and water samples; nearly 100 % recovery was achieved for hydroxychloroquine spiked into the water sample, while the amount of the labeled compound in the pharmaceutical tablet was accurately determined. This result confirmed that the multi-walled carbon nanotube-modified pencil graphite electrode is very effective for selectively and accurately determining hydroxychloroquine in real samples.

Keywords: Differential pulse voltammetry, Electrochemical detection, Hydroxychloroquine, Multi-walled carbon nanotube, Pencil graphite electrode.

1. Introduction

COVID-19, SARS-CoV-2, which first appeared in Wuhan, China, in December 2019, has evolved into variants such as Delta, Omicron, and Ba.2 over time and has caused the death of many people between 2019 and 2023. The COVID-19 outbreak was declared a global pandemic by the World Health Organization (WHO) on March 11, 2020 [1]. According to WHO reports, there have been more than 777.7 million cases and more than 7 million deaths to date. [2]. In the early days of COVID-19, researchers tested several existing antiviral drugs that have been proven effective and safe against viruses for the treatment of COVID-19. Although vaccine studies were quickly initiated in the following years and COVID-19 began to be controlled with these vaccines, some antiviral drugs were extensively used in the early periods.

In the treatment of COVID-19, various alternatives have been used, including antiviral, anti-inflammatory, and anti-rheumatic drugs; plasma; hyperimmune immunoglobulins; and low molecular weight heparins, especially for patients with moderate to severe cases, depending on their health condition and the various stages of disease [3]. One of the antiviral drugs used for this purpose is 4-aminoquinolines. Chloroquine and hydroxychloroquine (HCQ) as 4-aminoquinolines increase antiviral activity with a synergistic effect due to having both antiviral and immunomodulatory functions.

For this reason, it has been widely used in the prophylaxis and treatment of malaria and in the treatment of many chronic diseases such as rheumatoid arthritis and systemic lupus erythematosus [3-5]. The mechanism of action of these compounds has been attributed to lysosomal acidification and protein degradation, since these weak bases increase the pH of the endosomes used by the virus for cell entry. This pH increase leads to the prevention of autophagosome-lysosome fusion and inactivation of enzymes that viruses need for replication [4, 6-7]. Additionally, inhibition of phospholipase and interleukins (IL-1, IL-6) and tumor necrosis factor (TNF)-alpha have also been postulated as causal mechanisms [5]. It has also been predicted that HCQ, which has been associated with interfering with the glycosylation of angiotensin-converting enzyme2 (ACE2), the cellular receptor of SARS-CoV, and related gangliosides, could also be used in the treatment of COVID-19 [7]. On the other hand, it has been reported that the risk of ventricular arrhythmias and death in the hospital increases as a result of the use of these drugs in patients, and that this event is associated with the cardiovascular toxicity of chloroquine or HCQ [3, 8]. As a result of the clinical studies conducted, the WHO announced on June 17, 2020, that the HCQ arm of the Solidarity trial project to find an effective treatment against COVID-19 was stopped [3, 8].

Therefore, the detection of HCQ in both biological samples and pharmaceutical tablets is of extreme importance. For this purpose, spectrophotometric [9, 10], spectrofluorimetric [11, 12], chromatographic [13-16], capillary electrophoresis [17], and electrochemical methods [18-30] have been developed for the determination of HCQ. Among these, electroanalytical methods are widely used in pharmaceutical studies because they offer numerous advantages such as ease of use, simplicity, lower cost compared to other methods, rapid response, suitability for miniaturization and portability, acceptable accuracy, precision, sensitivity, and selectivity [31-34]. In this context, various types of modified electrodes, such as cathodically pretreated boron-doped diamond electrode [18], carbon black Super P modified glassy carbon electrode [20], 3D printed carbon black-polylactic acid electrode [22], Pt nanoparticles and multi-walled carbon nanotube (MWCNT) modified carbon paste electrode [23], natural phosphate modified graphite paste electrode [24], and sodium dodecyl sulfate modified carbon nanotube paste electrode [26], have been proposed for sensitive and selective determination of HCQ. However, according to our literature research, an HCQ determination based on the use of a pencil graphite electrode (PGE) has not yet been performed.

Compared to other solid carbon-based electrodes, PGE has some advantages, such as not requiring time-consuming preparation and cleaning steps, being easily available commercially, being simple to use, being disposable, having a wide working potential range, and being relatively inexpensive. Due to these properties, many electrochemical studies based on the use of PGE have been carried out in recent years [35-40]. In this study, investigation of the electrochemical behavior of HCQ and its differential pulse voltammetric determination have been performed using MWCNT-modified PGE for the first time.

2. Materials and Methods

2.1. Chemicals and Apparatus

Hydroxychloroquine sulfate (98.6% purity) was supplied by Neutec Pharmaceutical Company (İstanbul, Türkiye). Its stock solution (0.01 $molL^{-1}$) was prepared daily by dissolving an appropriate amount of its solid in ultra-pure water, and the final volume of the solution was diluted to 5.0 mL with ultra-pure water. Other reagents such as H_3PO_4, H_3BO_3, CH_3COOH, NaOH, KCl, and some compounds used in the interference study (ascorbic acid, dopamine, uric acid, and glucose) were purchased from Sigma Aldrich. To prepare stock and standard solutions, ultrapure water (18.2 $M\Omega\ cm^{-1}$) produced by an Elga Option Q7B water purification system was used.

Britton-Robinson buffer (BRB) solutions, including 0.1 $molL^{-1}$ KCl used as the supporting electrolyte, were prepared by mixing a 0.04 $molL^{-1}$ acid solution (H_3PO_4, H_3BO_3, CH_3COOH) with a base solution (0.2 $molL^{-1}$ NaOH). The pHs of BRB solutions between 6.0 and 10.0 were adjusted with a pH meter (Hanna HI 221 pH meter).

A Galvanoplot brand GX203 model compact potentiostat (İzmir, Türkiye) device was used for electrochemical studies. The electrochemical measurements were performed by using a conventional three-electrodes system including TOMBOW 2B 0.5 mm (Japan) pencil leads as a working electrode, Ag/AgCl (sat. KCl) as a reference electrode, and Pt wire as the counter electrode. The length of pencil leads immersed in the supporting electrolyte was arranged as 1 cm (the geometric area of 0.159 cm^2) with a ruler. The MWCNT modified pencil leads were placed in a Rotring pen holder, the metal part was adjusted to connect to the working electrode socket of the galvanostat with a Cu wire before use (Figure 1). A JEOL JSM-7100-F scanning electron microscopy (SEM) device at the Science and Technology Application and Research Center (ÇOBİLTUM) of Çanakkale Onsekiz Mart University was used for the surface characterizations of bare PGE and MWCNT-modified PGE.

2.2. Preparation of MWCNT/PGE and Electrochemical Measurements

To prepare the MWCNT modified electrode, an acid functionalized MWCNT suspension of 2.0 $mgmL^{-1}$ was prepared in dimethylformamide (DMF). An acid

functionalization procedure reported in a previous study procedure was also used in this study [35]. To prepare the MWCNT modified PGE, pencil leads were dipped into this 2 mgmL^{-1} MWCNT suspension twice for 5 min in total and dried under an IR lamp (Medisana IRL, Germany, 230 V, ~50 Hz and 150 W). In the preparation step, the time and numbers of immersions of electrodes into the MWCNT suspension were optimized by recording the cyclic voltammograms (CVs) of HCQ.

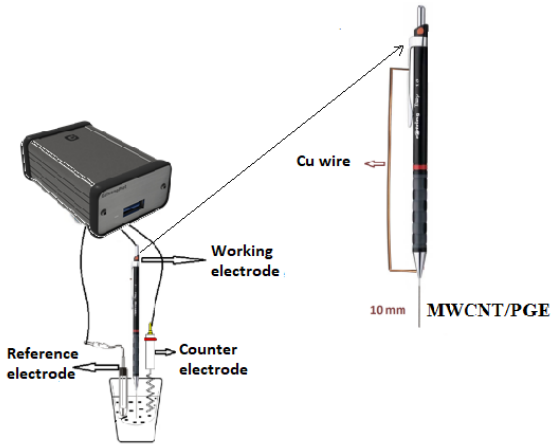

Figure 1. Galvanostat and three-electrode system including MWCNT/PGE as working electrode.

To investigate the electrochemical behavior of HCQ, CVs of 5.0x10^{-4} molL^{-1} HCQ were recorded in BRB solutions containing 0.10 molL^{-1} KCl with varied pH in the range from 6.0 to 11.0 at a scan rate of 50 mVs^{-1} in the potential range from -500 mV to +1200 mV. Then, CVs of 5.0x10^{-4} molL^{-1} HCQ were recorded at scan rates varying in range from 20 to 600 mVs^{-1} at pH 10.0 BRB solution containing 0.10 molL^{-1} KCl in the same potential range.

To determine analytical performance parameters, the differential pulse voltammograms (DPVs) of HCQ were recorded. The DP voltammetric parameters, such as potential step (E_{Step}), pulse amplitude (E_{Amp}), and pulse time (t_{Pulse}), that affect the intensity of the electrochemical signal of HCQ were optimized. For this aim, DPVs of 50 µmolL^{-1} HCQ were recorded based on each varied parameter in pH 10.0 BRB solution containing 0.10 molL^{-1} KCl. Then, oxidation peak currents of HCQ versus its concentration were monitored by recording DPVs under optimized conditions.

2.3. Real Sample Studies

The practical feasibility of the DP voltammetric method proposed for the determination of HCQ was tested on tap water samples that were taken from the laboratory of the Chemistry Department and on commercially purchased pharmaceutical tablets containing 200 mg of HCQ per tablet. Firstly, tap water samples were spiked to contain three different concentrations of HCQ (0.5, 5.0 and 10.0 µmolL^{-1}). Then, the pH 10.0 BRB solutions containing 0.10 molL^{-1} KCl were prepared from these spiked solutions, and DPVs of each spiked solution were recorded under optimized conditions. Next, known volumes of HCQ stock solution were sequentially added to the cell containing already spiked water samples, and DPVs were recorded after each standard addition. To determine HCQ in the pharmaceutical sample, a tablet containing 200 mg of HCQ was first ground into powder in a porcelain mortar, then dissolved in methanol, and diluted to a final volume of 10.0 mL. Then, a background voltammogram of MWCNT/PGE was recorded in 5.0 mL of pH 10.0 BRB solution containing 0.10 molL^{-1} KCl. Further, an appropriate volume of diluted pharmaceutical solutions was added to the supporting electrolyte, and DPVs were recorded under optimized conditions. This was followed by the standard addition method as mentioned for spiked water samples.

3. Results and Discussion

3.1. Preparation and Characterization of MWCNT/PGE

To prepare the modified electrode, one cm of the 5 cm long pencil leads was immersed into the 2 mgmL^{-1} MWCNT suspension prepared in DMF. After 5 min, the MWCNT-covered pencil leads were removed from the suspension and dried immediately under the IR lamp. This procedure was repeated twice in total. Surface characterization of bare PGE and MWCNT/PGE was examined by recording their SEM images. Figures 2A and 2B show the SEM images of PGE and MWCNT/PGE, respectively. It is seen from the figure that the smooth and layered structures of the graphite pencil leads are covered with carbon nanotube fibers. This figure proves that the PGE surface is coated with MWCNT.

Celal Bayar University Journal of Science
Volume 21, Issue 3, 2025, p 121-130
Doi: 10.18466/cbayarfbe.1705373

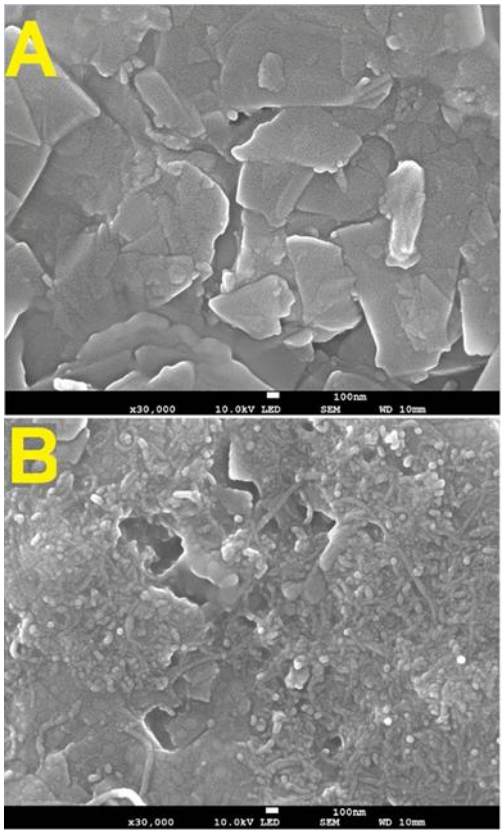

Figure 2. The SEM images of bare PGE (A) and MWCNT/PGE (B).

3.2. Electrochemical Behavior of HCQ at MWCNT/PGE

To see the electrochemical behavior of HCQ at MWCNT/PGE, CVs of $5x10^{-4}$ $molL^{-1}$ HCQ were recorded at BRB solutions containing 0.10 $molL^{-1}$ KCl with pH ranging from 6.0 to 10.0 (Figure 3A). From CVs recorded, two oxidation peaks were observed at around 870 mV (denoted as Ox_I) and 1090 mV (denoted as Ox_{II}) at pH 6.0, and the peak potentials of these peaks shifted to more negative directions by increasing pH values. These results indicate that the electrochemical oxidation of HCQ at MWCNT/PGE occurs through a proton-coupled electron transfer reaction. On the other hand, any reduction peaks were not observed in the reverse scan because HCQ was irreversibly oxidized at MWCNT/PGE. Figure 3B shows that The highest peak currents for both oxidation peaks were obtained in the pH 10.0 BRB solution containing 0.10 $molL^{-1}$ KCl. Therefore, a pH 10.0 BRB solution containing 0.10 $molL^{-1}$ KCl was selected as the optimum supporting electrolyte in further studies.

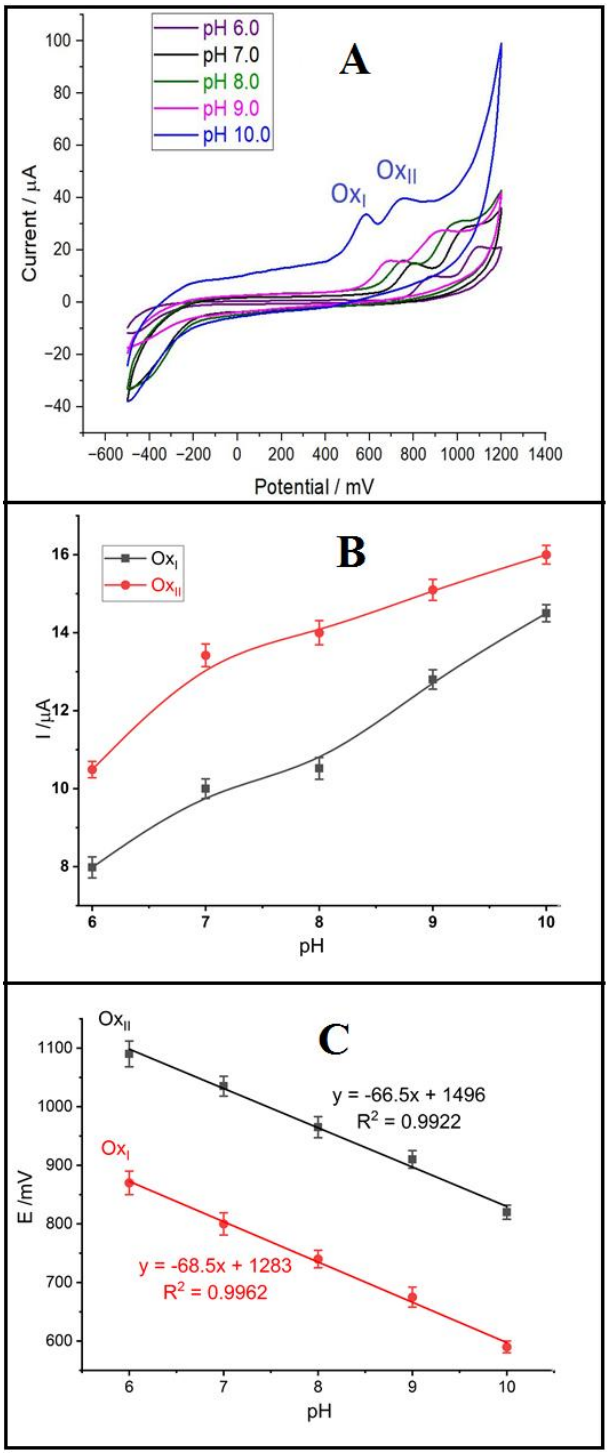

Figure 3. CVs of $5.0x10^{-4}$ $molL^{-1}$ HCQ at MWCNT/PGE in the BRB solutions containing 0.10 $molL^{-1}$ KCl with pH between 6.0 and 10.0 (scan rate = 50 mVs^{-1}) (A) and the curves of both oxidations peak currents (B) and potential (C) versus pH.

The graph of peak potentials (E(mV)) vs. pH is given in Figure 3B for both Ox_I and Ox_{II}. The curves of E(mV) versus pH were found to be linear for Ox_I and Ox_{II} between pH 6.0 and 10.0. Linear equations were estimated as E(mV) = -68.5×pH + 1283 and (E(mV) = -66.5×pH +1496 for Ox_I and Ox_{II}, respectively. These slopes of the obtained linear curves (-68.5 mV/pH for Ox_I and -66.5 mV/pH for Ox_{II}) are remarkably close to the theoretical Nernst value (~-59.0 mV/pH). This result reflects that the number of protons (H^+) is equal to the number of electrons (e^-) in the oxidation of HCQ [20, 22, 23]. The oxidation mechanism based on these results can be proposed as shown in Figure 4. A similar mechanism has been reported in the electrochemical oxidation of HCQ at several modified electrodes. According to the already reported studies in the literature and our results, Ox_I represents the oxidation of the primary alcohol to aldehyde by giving $2e^-$ and $2H^+$ [20, 23, 26]. Ox_{II} is attributed to the conversion of the N-heterocyclic nitrogen in the aminoquinoline moiety by the formation of a radical with one e^- and the delocalization of this radical into a cationic radical on the alkylamino nitrogen [28] and finally, the release of one H^+ resulted in the dimerization of HCQ by radical-radical coupling. The explanation that these two oxidation peaks are related to the deprotonation of amine and hydroxyl groups with pKa values < 8.3 and 9.7, respectively, supports this mechanism.

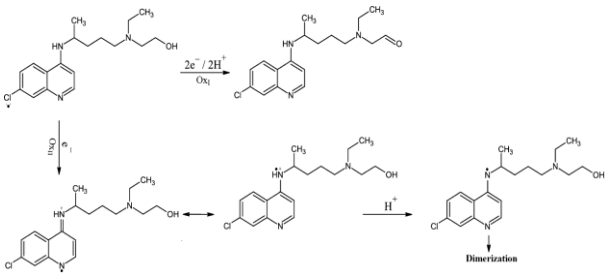

Figure 4. Oxidation mechanism of HCQ

To see the effect of scan rate on the oxidation of HCQ at MWCNT/PGE, the CVs of $5.0x10^{-4}$ $molL^{-1}$ HCQ were recorded at scan rates varying in the range from 10 to 600 mVs^{-1} in pH 10.0 BRB solution containing 0.10 $molL^{-1}$ KCl (Figure 5A). As the scan rate increased, a gradual increase in currents of both irreversible oxidation peaks of HCQ was observed. The graphs of current (I(μA)) vs. both scan rate (ν) and the square root of ν and the graph of log I(μA) vs. log ν were also given in Figures 5B-D. Figures 5B and 5C show that both Ox_I and Ox_{II} currents increase in a straight line with the square root of ν (not directly with ν), indicating that both oxidations of HCQ are controlled by a diffusion process rather than an adsorption process. In addition, the log I(μA)-log ν graphs (Figure 5D) support the diffusion-controlled process because the slopes of the curves (0.516 for Ox_I and 0.608 for Ox_{II}) are remarkably close to the theoretical slope value (0.50) for this type of process.

3.3. The Differential Pulse Voltammetric Determination of HCQ at MWCNT/PGE

To monitor differential pulse voltammetric responses of HCQ at MWCNT/PGE, some parameters such as pH, pulse amplitude, pulse time, and potential step were optimized by recording DPVs of 50 $\mu molL^{-1}$ HCQ. Results from recorded DPVs show that the highest peak currents for both Ox_I and Ox_{II} were obtained in the case of pH 10.0, 150 mV of pulse amplitude, 3 ms of pulse time, and 5.0 of step potential. Next, we conducted studies to evaluate the analytical performance of the method by recording the DPVs of HCQ at increasing concentrations in the range of 0.10-250 μM under these optimum conditions. The recorded DPVs and obtained calibration curves for both peaks are given in Figure 6. It can be seen from DPVs in Figure 6A and the calibration curve including a nonlinear part in Figure 6B that both Ox_I and Ox_{II} peaks are gradually increased by increasing the concentration of HCQ. Calibration curves for both Ox_I and Ox_{II} (Figures 6C and 6D) exhibit two linear regions in the range from 0.1 to 2.5 $\mu molL^{-1}$ and from 5.0 to 100 $\mu molL^{-1}$. The straight-line relationships for the two estimated concentration ranges were shown as equations: for Ox_I, I (μA) = 3.863 ($\mu molL^{-1}$) +1.433(R^2 = 0.9969) and I (μA) = 0.827C ($\mu molL^{-1}$) + 13.709 (R^2 = 0.9952); and for Ox_{II}, I (μA) = 3.145 ($\mu molL^{-1}$) + 1.4294 (R^2 = 0.9938) and I (μA) = 0.503C ($\mu molL^{-1}$) + 8.716 (R^2 = 0.9965). The sensitivity of the method was evaluated by estimation of the limit of detection (LOD) using the equation $3s.m^{-1}$ (s is the standard deviation of the current obtained for the lowest HCQ concentration at which a measurable signal is observed, and m is the slope of the first straight line of HCQ). The LOD values were estimated as 0.04 and 0.05 $\mu molL^{-1}$ for Ox_I and Ox_{II}, respectively.

Celal Bayar University Journal of Science
Volume 21, Issue 3, 2025, p 121-130
Doi: 10.18466/cbayarfbe.1705373

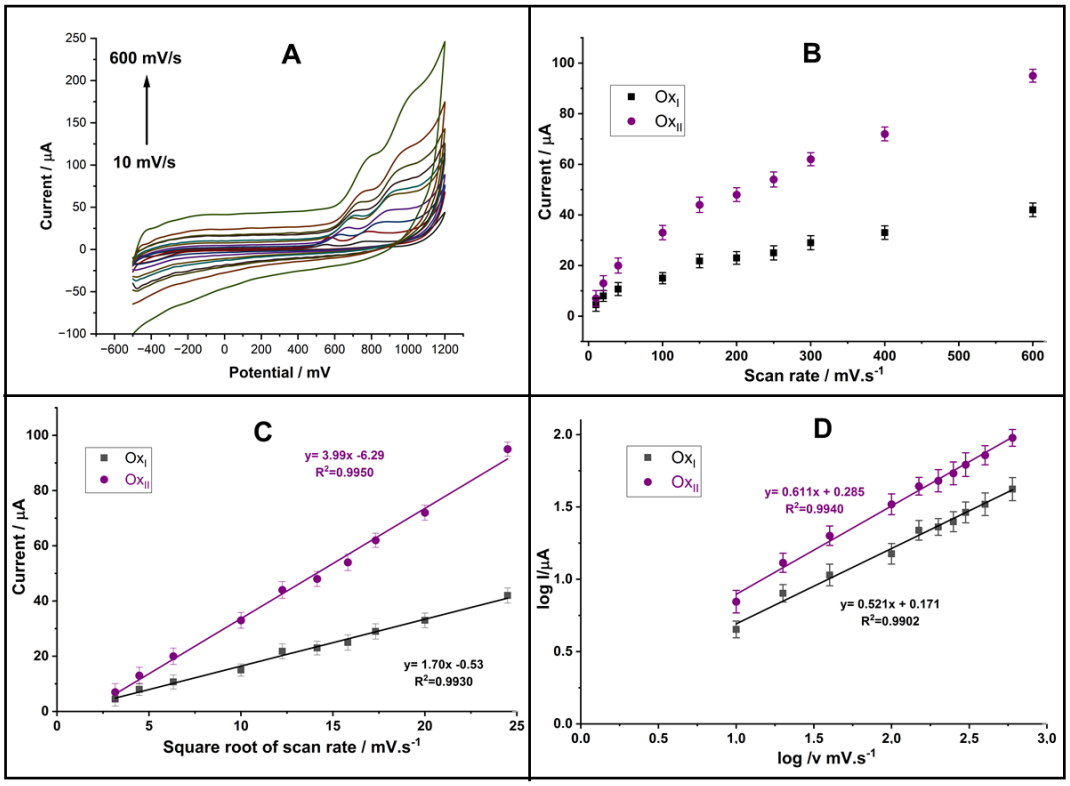

Figure 5. CVs of 5.0x10^{-4} molL^{-1} HCQ at MWCNT/PGE recorded at increasing scan rates in the range from 10 to 600 mVs^{-1} in pH 10.0 BRB solution containing 0.10 molL^{-1} KCl (A) and the curves of oxidation peaks versus scan rate (B) and square root of scan rate (C); and the curve of logarithmic peak currents versus logarithmic scan rate (D)

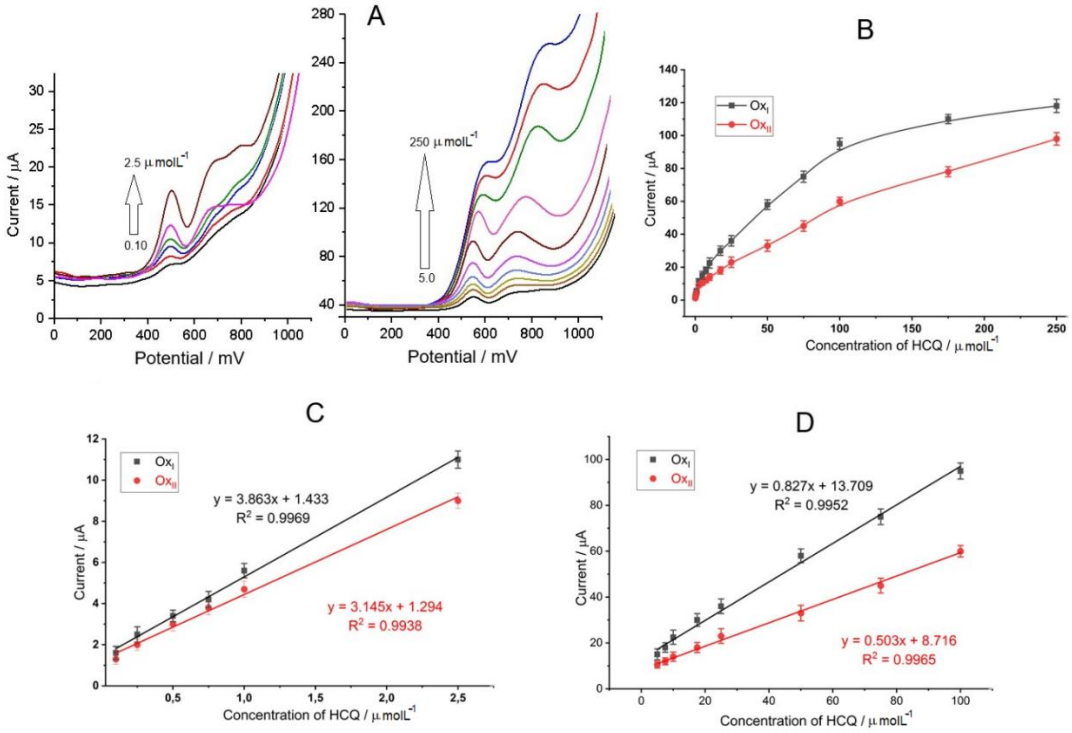

Figure 6. A) DPVs of HCQ recorded in the range from 0.1 to 250 µmolL^{-1} at MWCNT/PGE in pH 10.0 BRB solution containing 0.10 molL^{-1} KCl under optimized conditions. B) the curve of both oxidation peak currents vs. HCQ concentration; C) the first linear calibration plot in the range from 0.1 to 2.5 µmolL^{-1} HCQ; and D) the second linear calibration plot in the range from 5.0 to 100 µmolL^{-1} HCQ

The repeatability of MWCNT/PGE was investigated by recording three independent DPVs of the 50 µmolL^{-1} HCQ under optimal conditions for the same electrode. The average value and standard deviation for both Ox_I and Ox_{II} were calculated from their currents obtained from voltammograms. Then relative standard deviation (RSD) values were calculated as 2.58% and 2.91% for Ox_I and Ox_{II}, respectively. These results show that the voltammetric determination of HCQ at MWCNT/PGE has an acceptable precision.

To evaluate the analytical performance, Table 1 presents a comparison of MWCNT/PGE with some modified electrodes used in the electrochemical determination of HCQ. As shown in this table various types of modified electrodes were successfully used for the electrochemical determination of HCQ. The LOD values of MWCNT/PGE are lower than some of these studies; this indicates that the sensitivity of the proposed method is higher than the related studies. In addition, the sensitivity of the proposed method is competitive with some modified electrodes such as the 3D-printed carbon black-poly-lactic acid electrode [22], Pt-NPs-MWCNTs/CPE [23], AC-rGO@CPE [27] and cathodically pretreated boron-doped diamond electrode [18]. When we compare PGE with these modified electrodes, PGE shows some advantages, such as cost-effectiveness, commercial availability, ease of modification, good conductivity, disposability, and mechanical rigidity. In addition, PGE does not require the long-time and rigorous preparation steps, expensive modification materials, and hard cleaning and polishing steps of other carbon-based electrodes. It can be concluded that the proposed voltammetric determination approach using MWCNT/PGE has several advantages and exhibits promising performance in the determination of HCQ.

3.6. Interference Study

The effect of interference of some cationic and anionic species (K^+, Na^+, Mg^{2+}, Cu^{2+}, Ca^{2+}, Zn^{2+}, Ni^{2+}, Pb^{2+}, Cl^-, NO_3^- and SO_4^{2-}), and some electroactive compounds (dopamine (DA), uric acid (UA), and ascorbic acid (AA)) and non-electroactive glucose was investigated. For this aim, DPVs of 50 µmolL^{-1} HCQ were recorded in the absence and in the presence of possible interfering species by increasing the ratio of analyte to interfering species in the range from 1:1 to 1:100. The results show that cationic and anionic species do not affect both oxidation peak currents of HCQ in the ratio of 1:100. In addition, AA, DA, and UA are oxidized at 180 mV, -50 mV and +250 mV, respectively. Thus, AA does not give any interference effect on both oxidations of HCQ in a 1:20 ratio. Although DA is oxidized at more negative potential than HCQ, DA increased both oxidation peaks of HCQ in 1:5 ratios due to possible interaction between these two molecules. In the case of UA, Ox_{II} was not affected in the presence of a 1:50 ratio, while Ox_I was affected in the presence of 1:5 ratios due to overlapping peaks of UA and HCQ (only Ox_I). In the presence of glucose, both oxidations of HCQ were not affected in the presence of 1:100 ratios. These results show that the DP voltammetric method using MWCNT/PGE has high selectivity in the presence of the mentioned ratio of analyte to interferents for the determination of HCQ.

3.7. Application for Real Samples

To evaluate the applicability of this voltammetric procedure using MWCNT/PGE, firstly, a pharmaceutical tablet including 200 mg of HCQ was analyzed. For this purpose, DPVs of the tablet solution mentioned in the experimental section were recorded in pH 10.0 BRB solution containing 0.10 molL^{-1} KCl under the optimized conditions. Then, the standard addition procedure was applied to determine the level of HCQ in the pharmaceutical sample. The value of HCQ in the pharmaceutical tablet was found to be 205 mg ± 8 with an RSD of 3.9%. This result reflects that HCQ in the pharmaceutical tablets can be determined with adequate accuracy and precision.

As a second sample, tap water was spiked with three different concentrations of HCQ (0.5, 5.0, and 10.0 µmolL^{-1}). Firstly, DPVs of each spiked sample were recorded, and then the standard addition method was used. Table 2 presents the recovery results from the tap water sample. The recovery values, which range from 99.3 % to 104.7 %, show that the suggested voltammetric method works well for accurately and sensitively determining HCQ in water samples.

Table 1. A comparison of the analytical performance of MWCNT/PGE with previously reported modified electrodes in the literature for electrochemical determination of HCQ

Electrode material	***Electrochemical technique***	***Linear range*** (μmolL^{-1})	***LOD*** (μmolL^{-1})	***Sensitivity*** µALµmol^{-1}	***The samples used in applicability***	***Ref.***
3D-printed CB-PLA electrode	SWV	0.4-7.5 (Ox_{II})	0.04	0.28	Tap water and pharmaceutical tablet	22
Pt NPs-MWCNTs/CPE	SWV	0.099–7.1 (Ox_{II})	0.028	0.20	River water, synthetic urine, and bovine serum	23
NPh–CPE	DPV	0.8-10 (Ox_I) 0.4-10 (Ox_{II})	0.527 (Ox_I) 0.334 (Ox_{II})	1.51x10^{-4} (Ox_I) 2.38x10^{-4} (Ox_{II})	Blood and pharmaceutical tablet	24
GC-PMPDA SAM modified electrode	DPV	1st region = 0.05–12.28 (Ox_{II}) 2nd region =12.28–111.11 (Ox_{II})	4.51x10^{-3}	0.2079 and 0.0087	Human blood serum	25
SPCB/GCE	LSV	1st region = 0.10-1.0 (Ox_{II}) 2nd region = 1.0-10 (Ox_{II})	0.093	4.6 and 3.2	Tap water and pharmaceutical tablet	20
SDSMCNTPE	CV	10-40 (Ox_I)	0.85	0.2929	Pharmaceutical tablet	26
AC−rGO@CPE	DPV	0.40-4.0	0.032	-	Human urine and wastewater.	27
MWCNT/ITO	Amp at +1.1 V	1.0-100	0.26	0.131	Tap water and river	28
CPT-BDDE	SWV	0.10–1.90	0.06	1.24	Pharmaceutical tablet	18
ZnO@CPE	SWV	0.8-1000	0.133	4.52	Tap wate and human urine	30
MWCNT/PGE	*DPV*	*1st region = 0.1-2.5 (Ox_I and Ox_{II})* *2nd region = 5-100 (Ox_I and Ox_{II})*	*0.04 (Ox_I) 0.05 (Ox_{II})*	*3.863 and 0.827 (Ox_I) 3.145 and 0.503 (Ox_{II})*	*Tap water and pharmaceutical tablet*	*This work*

Table 2. The results obtained from tap water sample (n= 3).

Sample	***Added HCQ (μmolL^{-1})***	***Found HCQ (μmolL^{-1})***	***Recovery %***	***RSD %***
Tap water	0.5	0.48 ± 0.025	96.0	5.2
	5.0	5.46 ± 0.24	109.2	4.4
	10.0	10.37 ± 0.40	103.7	3.9
Tablet	***Labelled amount***	***Found HCQ***	***Bias %***	***RSD %***
	200 mg	205 mg ± 8	*2.5*	*3.9*

4. Conclusion

This study shows that the MWCNT/PGE has been used for sensitive and selective voltammetric determination of HCQ. MWCNT/PGE offers some advantages, such as disposability, cost-effectiveness, commercial availability, and a highly conductive surface. The modified electrode shows two peaks for HCQ oxidation at about +650 and +900 mV in pH 10 BRB solution containing 0.10 molL^{-1} KCl. Both of these oxidation peaks have two linear calibration ranges between 0.10 and 2.5 µmolL^{-1} and between 5.0 and 100 µmolL^{-1} HCQ with the LOD values of 0.04 and 0.05 µmolL^{-1}, respectively. The results from the application studies show that HCQ can be accurately determined in the pharmaceutical tablet, including 200 mg of HCQ per tablet. Also, good recovery results were found in tap water samples that had known amounts of HCQ added,

showing that the method can accurately measure HCQ in water samples. The specificity of this study is that the electrochemical sensor designed for HCQ demonstrates excellent disposability and cost-effectiveness, both of which are important features for practical applications.

Acknowledgement

The authors thank Prof. Dr. Yusuf Dilgin for his technical assistance and the source of special materials.

Author's Contributions

Sultan Hasankahyaoğlu: Investigation, Conceptualization, Data curation

Şevval Sazlık: Investigation, Conceptualization, Data curation

İrem Demir: Validation, Methodology, Visualization

Selen Ayaz: Investigation, Data curation, Writing-original draft

Didem Giray Dilgin: Data curation, Supervision, Writing – review & editing

Ethics

This study does not require any ethical approval.

References

[1]. WHO, WHO Director-General's opening remarks at the media briefing on COVID-19. https://www.who.int/director-general/speeches/detail/who-director-general-s-opening-remarks-at-the-media-briefing-on-covid-19---11-march-2020/, 11 Mach 2020 (accessed at 23.05.2025).

[2]. WHO, WHO Coronavirus (COVID-19) Dashboard. https://covid19.who.int/, 9 November 2022 (accessed at 23.05.2025).

[3]. Stasi, C, Fallani, S, Voller, F, Silvestri, C. 2020. Treatment for COVID-19: An overview. *European Journal of Pharmacology*; 889: 173644.

[4]. Sinha, N, Balayla, G. 2020. Hydroxychloroquine and COVID-19. *Postgraduate Medical Journal*; 96: 550–555.

[5]. Fox, RI. 1993. Mechanism of action of hydroxychloroquine as an antirheumatic drug. *Seminars in Arthritis and Rheumatism*; 23(2): 82-91.

[6]. Ferner, RE, Aronson, JK. 2020. Chloroquine and hydroxychloroquine in COVID-19. *BMJ*; 369: m1432.

[7]. The RECOVERY Collaborative Group. 2020. Effect of hydroxychloroquine in hospitalized patients with COVID-19. *The New England Journal of Medicine*; 383(21): 2030-2040.

[8]. WHO, WHO solidarity trial consortium, repurposed antiviral drugs for COVID-19 — interim who solidarity trial results. 2021. *The New England Journal of Medicine*; 384(6): 497-511.

[9]. Bhati, KN, Mashru, R. 2022. Development and validation of extractive spectrophotometric method for estimation of hydroxychloroquine sulphate by using smartphone application. *Journal of Drug Delivery & Therapeutics*; 12(3): 49-56.

[10]. Sura, SALD, Samarray, SYAL. 2022. Determination spectrophotometric and cloud point extraction of hydroxychloroquine sulfate. *HIV Nursing*; 22(2): 2900-2904.

[11]. Ramzy, S, Abdelazim, AH, Osman, AOE, Hasan, MA. 2022. Spectrofluorimetric quantitative analysis of favipiravir, remdesivir and hydroxychloroquine in spiked human plasma. *Spectrochimica Acta Part A: Molecular and Biomolecular Spectroscopy;* 281: 121625.

[12]. El Sharkasy, ME, Tolba, MM, Belal, F, Walash, M, Aboshabana, R. 2022. Quantitative analysis of favipiravir and hydroxychloroquine asFDA-approved drugs for treatment of COVID-19 usingsynchronous spectrofluorimetry: application to pharmaceuticalformulations and biological fluids. *Luminescence*; 37: 953-964.

[13]. Bodur, S, Erarpat, S, Günkara, OT, Bakırdere, B. 2021. Accurate and sensitive determination of hydroxychloroquine sulfate used on COVID-19 patients in human urine, serum and saliva samples by GC-MS. *Journal of Pharmaceutical Analysis*; 11: 278-283.

[14]. Sok, V, Marzan, F, Gingrich, D, Aweeka, F, Huang, L. 2021. Development and validation of an LC-MS/MS method for determination of hydroxychloroquine, its two metabolites, and azithromycin in EDTA-treated human plasma. *PLoS ONE*; 16(3): e0247356.

[15]. Volin, P. 1995. Simple and specific reversed-phase liquid chromatographic method with diode-array detection for simultaneous determination of serum hydroxychloroquine, chloroquine and some corticosteroids. *Journal of Chromatography B*; 666: 347-353.

[16]. Bilgin, ZD, Evcil, I, Yazgi, D, Binay, G, Genc, CO, Gulsen, B, Huseynova, A, Ozdemir, AZ, Ozmen, E, Usta, Y, Ustun, S, Andac, SC. 2021. Liquid chromatographic methods for COVID-19 drugs, hydroxychloroquine and chloroquine. *Journal of Chromatographic Science*; 59(8): 748-757.

[17]. Oliveira, ARM, Cardoso, CD, Bonato, PS. 2007. Stereoselective determination ofhydroxychloroquine and its metabolitesin human urine by liquid-phasemicroextraction and CE. *Electrophoresis*; 28: 1081-1091.

[18]. Deroco, PB, Vicentini, FC, Oliveira, GG, Rocha-Filho, RC, Fatibello-Filho, O. 2014. Square-wave voltammetric determination of hydroxychloroquine in pharmaceutical and synthetic urine samples using a cathodically pretreated boron-doped diamond electrode. *Journal of Electroanalytical Chemistry*; 719: 19-23.

[19]. de Araújo, DM, Paiva, SDSM, Henrique, JMM, Martínez-Huitle, CA, Dos Santos, EV. 2021. Green composite sensor for monitoring hydroxychloroquine in different water matrix. *Materials*; 14: 4990.

[20]. Silva, JPC, Neto, DRS, Lopes, CEC, Silva, LRG, Dantas, LMF, da Silva, IS. 2025. A high sensitivity adsorptive electrochemical method for rapid and portable determination of hydroxychloroquine. *Journal of Solid State Electrochemistry*; 29: 1013-1023.

[21]. Arguelho, MLPM, Andrade, JF, Stradiotto, NR. 2023. Electrochemical study of hydroxychloroquine and its determination in plaquenil by differential pulse voltammetry. *Journal of Pharmaceutical and Biomedical Analysis*; 32: 269-275.

[22]. Carvalho, MS, Rocha, RG, de Faria, LV, Richter, EM, Dantas, LMF, da Silva, IS, Munoz, RAA. 2022. Additively manufactured electrodes for the electrochemical detection of hydroxychloroquine. *Talanta*; 250: 123727.

[23]. Feitosa, MHA, Santos, AM, Wong, A, Sotomayor, MDPT, Barros, WRP, Lanza, MRV, Moraes, FC. 2025. Enhancing hydroxychloroquine detection using carbon paste electrode modifed

with platinum nanoparticles and MWCNTs. *Journal of Applied Electrochemistry*; 55: 2265-2276.

[24]. Matrouf, M, Loudiki, A, Azriouil, M, Laghrib, F, Ait Akbour, R, Farahi, A, Bakasse, M, Saqrane, S, Lahrich, S, El Mhammedi, MA. 2022. Electrochemical behavior of hydroxychloroquine on natural phosphate and its determination in pharmaceuticals and biological media. *Materials Chemistry and Physics*; 287: 126340.

[25]. Khoobi, A, Ghoreishi, SM, Behpour, M, Shaterian, M, Salavati-Niasari, M. 2014. Design and evaluation of a highly sensitive nanostructure-based surface modification of glassy carbon electrode for electrochemical studies of hydroxychloroquine in the presence of acetaminophen. *Colloids and Surfaces B: Biointerfaces*; 123: 648-656.

[26]. Pushpanjali, PA, Manjunatha, JG, Hareesha, N, Girish, T, Al Kahtani, AA, Tighezza, AM, Ataollahi, N. 2025. Electrocatalytic determination of hydroxychloroquine using sodium dodecyl sulphate modifed carbon nanotube paste electrode. *Topics in Catalysis*; 8, 1373-1381.

[27]. Matrouf, M, Loudiki, A, Ouatmane, FZ, Chhaibi, B, Alaoui, OT, Laghrib, F, Farahi, A, Bakasse, M, Lahrich, S, El Mhammedi, MA. 2022. Effect of graphite exfoliation way on the efficiency of exfoliated graphene for the determination of hydroxychloroquine in urine and waste water. *Journal of the Electrochemical Society;* 169: 097505.

[28]. Silva, MNT, Alves, DAC, Richter, EM, Munoz, RAA, Nossol, E. 2023. A simple, fast, portable and selective system using carbon nanotubes films and a 3D-printed device for monitoring hydroxychloroquine in environmental samples. *Talanta*; 265: 124810.

[29]. Khalil, MM, Issab YM, El Sayeda GA. 2015. Modified carbon paste and polymeric membrane electrodes for determination of hydroxychloroquine sulfate in pharmaceutical preparations and human urine. *RSC Advances*; 5: 83657-83667.

[30]. Zoubir, J, Bakas, I, Qourza, S, Tamimi, M, Assabbane, A. 2023. Electrochemical sensor based on a ZnO doped graphitized carbon for the electrocatalytic detection of the antibiotic hydroxychloroquine. Application: tap water and human urine. *Journal of Applied Electrochemistry*; 53: 1279-1294.

[31]. Vural, K, Karakaya, S, Dilgin, DG, Gokçel, HI, Dilgin, Y. 2023. Voltammetric determination of Molnupiravir used in treatment of the COVID-19 at magnetite nanoparticle modified carbon paste electrode. *Microchemical Journal*; 184: 108195.

[32]. David, IG, Buleandra, M, Popa, DE, Cheregi, MC, David, V, Iorgulescu, EE, Tartareanu, G.O. 2022. Recent developments in voltammetric analysis of pharmaceuticals using disposable pencil graphite electrodes. *Processes*; 10: 472.

[33]. Günes, M, Karakaya, S, Kocaaga, T, Yıldırım, F, Dilgin, Y. 2021. Sensitive voltammetric determination of oxymetazoline hydrochloride at a disposable electrode. *Monatshefte für Chemie - Chemical Monthly*; 152: 1505-1513.

[34]. Brycht, M, Konecka, K, Sipa, K, Skrzypek, S, Mirˇceski, V. 2019. Electroanalysis of the anthelmintic drug bithionol at edge plane pyrolytic graphite electrode. *Electroanalysis*; 31: 2246–2253.

[35]. Karakaya, S, Dilgin, Y. 2023. The application of multi walled carbon nanotubes modifed pencil graphite electrode for voltammetric determination of favipiravir used in COVID 19 treatment. *Monatshefte für Chemie - Chemical Monthly*; 154: 729-739.